Synthesis and Characterization of Stable Organosols of Silver Nanoparticles by Electrochemical Dissolution of Silver in DMSO

Mihir M. Wadkar, Vijay R. Chaudhari, and Santosh K. Haram*

Department of Chemistry, University of Pune, Ganeshkhind, Pune 411007, India

Received: June 2, 2006; In Final Form: August 15, 2006

Stable organosols of silver nanoparticles (AgNPs) without any capping agents have been synthesized by an electrochemical dissolution of a sacrificing silver electrode in dimethyl sulfoxide (DMSO). The peak at 425 ± 5 nm observed in the UV−vis spectra was attributed to the surface plasmon resonance for silver. The formation of nanoparticles of silver was confirmed by X-ray diffraction analysis (XRD). In TEM, three ranges of particle size were observed, namely, 3.75 ± 0.8, 6.25 ± 0.5, and 9.25 ± 0.3 nm. The correlation among these sizes was explained by a new model based on a droplet coalition. Based on that, sizes correlation fits very well in the empirical formula $5d_1^3n' + (3 - n')d_2^3 = d_3^3$ where d_1, d_2, and d_3 are three sizes of particles and n' is an integer having values 0, 1, 2, 3, ... The sols prepared in DMSO were stable against flocculation for months. An unusual solution stability without any capping agents was attributed to the formation of Ag(I)DMSO complex on particle surface, which was confirmed by FTIR, fluorescence spectroscopy, and thermal analysis.

1. Introduction

Nanoparticles (NPs) of metals, especially noble metals, have gained a considerable interest in recent years due to their immense applications in optoelectronics,[1,2] catalysis,[3] mechanics,[4] drug delivery, immuno-assay,[5] information storage,[6−11] and energy conversion.[12,13] Electronic properties of these nanoparticles are greatly influenced by shapes, size, and surface modifications. Therefore, emphasis has been given to prepare NPs having a control over these properties. Among various chemical routes developed for synthesis, the most common one is reducing the metal salts with sodium citrate[14] and sodium borohydride,[15] in the presence of surfactants or capping agents in a single phase or two immiscible phases having a phase transfer catalyst.[16] However, difficulties have been encountered in isolating these particles from other byproducts or surfactants used. Thus, an emphasis has been given to use a minimum number of reagents. For example, metal salts have been reduced by solvent itself, instead of using separate reducing agents. Poly(*N*-vinyl-2-pyrrolidone), dry ethanol, methanol, *N*′,*N*′-dimethylformamide,[17] and DMSO[18] have been tried for this purpose.

The electrochemical method provides a viable route to produce metal NPs, without use of any reducing agent that may further improve the purity. The particle size is controlled by simple variables such as current and overpotential.[19] Yin et al.[20] describes the preparation of AgNPs by electroreduction of $AgNO_3$ on the Pt electrode in the presence of poly(*N*-vinylpyrrolidone). The mechanism of the formation was described in terms of a reduction of Ag_m^{n+}-PVP complex to Ag^o-PVP adatoms. The method was further modified by Ma et al.,[21] where better size control on PVP stabilized Ag and AuNPs has been reported by a controlled convection with the help of a rotating disk cathode. Metal carbonyl precursors also have been used to produced a composite of Pd, Ru, and Rh nanoparticles with pyrrole.[22] Socol et al.[23] used a sonoelectrochemical method in which electrodeposited Ag on Ti horn was detached periodically in the form of NPs by synchronized sonicating pulse.

Yet another electrochemical strategy has been suggested by Reetz et al. in which palladium NPs were produced by electrochemical dissolution of sacrificing Pd anode in the presence of tetraoctylammonium bromide.[19] This method further minimizes the reagents used for the synthesis, thus providing a possibility to deliver extremely pure sols on a large scale. The method has been extended further to prepare nanoparticles and nanorods of Ag[24] and Au.[25]

In the case of electrochemical synthesis of PdNPs, Reetz et al. demonstrated that particle size is an inverse function of applied overpotential.[19] That means the smallest possible particle size may be obtained by applying higher overpotentials. However, this possibility has not yet been reported. Perhaps one of the reasons could be a compitative reduction/oxidation of supporting electrolyte/capping agents themself at very high overpotentials. Therefore, it would be interesting to consider the preparation of AgNPs at higher overpotential values without any supporting electrolyte or capping agents. We observed that the sols obtained under these conditions were extremely stable against flocculation, despite the absence of capping agents. The particle with three different size distributions was observed in TEM. A new model is suggested to explain rational correlation among these sizes. FTIR spectra recorded on NPs suggested the formation of a Ag(I) DMSO complex on the particle surface, which is responsible for an unusual solution stability. Higher potential difference (100 V) presumingly facilitated the formation of this complex on the surface through electron transfer reactions. The mechanism of its formation is not yet clearly understood by us.

2. Experimental Section

2.1. Materials. All the chemicals were of Analytical Reagent (AR) grade and used as received. Dimethyl sulfoxide (DMSO)

* To whom correspondence to be addressed. E-mail: haram@chem.unipune.ernet.in. Fax: +912025693981.

10.1021/jp063422p CCC: $33.50 © 2006 American Chemical Society
Published on Web 09/27/2006

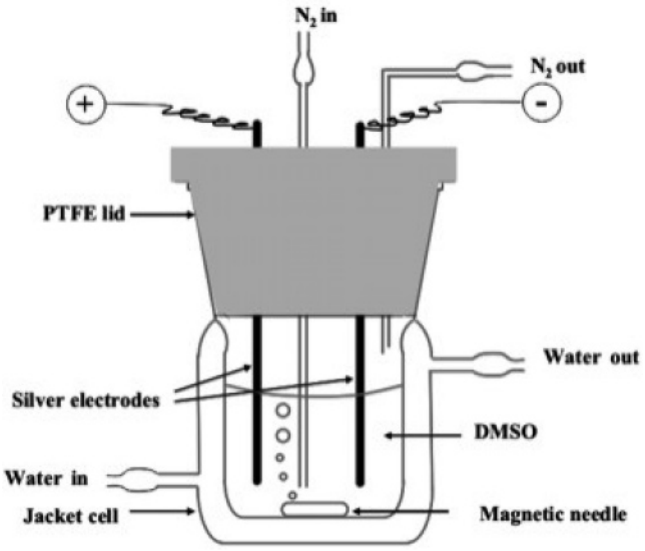

Figure 1. A sketch of two-electrodes cell used for the synthesis of Ag nanoparticles sols in DMSO. The volume of the cell was 150 mL. The separation between the two electrodes (diameter 2 mm) was kept at 2 cm. The temperature of the cell was maintained at 28 °C by using a water circulating thermostatic bath.

and dimethylformamide (DMF) (water content less than 0.03%) were purchased from SD's Fine chemicals, India. Two silver electrodes (99%) of identical size (2.0 mm diameter) were used as cathode and anode. Some reactions were carried out in N_2 atmosphere (Indian Oxygen Ltd, IOLAR grade, O_2 less than 5 ppm). Few experiments were performed with platinum electrodes of similar area.

2.2. Electrolysis with Silver Electrode in DMSO. The setup used for the electrolysis is described in Figure 1. In brief, the electrolysis was carried out in a cylindrical jacket cell (volume ca. 150 cm^3), with an airtight PTFE stopper. Two silver rod electrodes of identical size (diameter 2.0 mm, contact length 30 mm, and geometrical contact area ca. 192 mm^2) were fitted vertically in the cell. The distance between these electrodes was kept at 2.0 cm. The temperature of the cell was maintained by using a thermostated circulating bath set at 28 ± 0.2 °C. Prior to the reaction, the electrodes were polished with a fine emery paper, subsequently rinsed with copious amount of double distilled water, and dried under vacuum.

Typically, 100 mL of DMSO was transferred into the cell and solutions were degassed by using N_2 bubbling for ca. 10 min. Next 100 V was applied between these electrodes with continuous stirring. The electrolysis was carried out at controlled potential mode with an observed current density in the range 200−260 mA cm^{-2}.

As electrolysis proceeded, the color of the solution changed from colorless to pale yellow, due to the formation of silver NPs. After a stipulated time (ca. 50 min), the power supply was switched off and the resultant sol was transferred into an Amber colored stoppered bottle. In the dark, these sols were found to be stable for more than eight months without losing much of their optical characteristics. In contrast, The sols prepared in the potential ranges 50 and 150 V showed poor yield and low solution stability, respectively (refer to the Supporting Information).

2.3. Extraction of NPs from Sols. Powder samples for material characterization were obtained by flocculating the sols, using acetone as an antisolvent. Typically, 20 mL of acetone was required for the first appearance of turbidity. The particles were allowed to settle overnight, then separated by centrifugation at 8000 rpm (15 min) followed by decantation. The resulting flocculate was washed several times with a copious amount of acetone, dried, and stored under vacuum for further analysis. The dried sols were readily redispersable in DMSO.

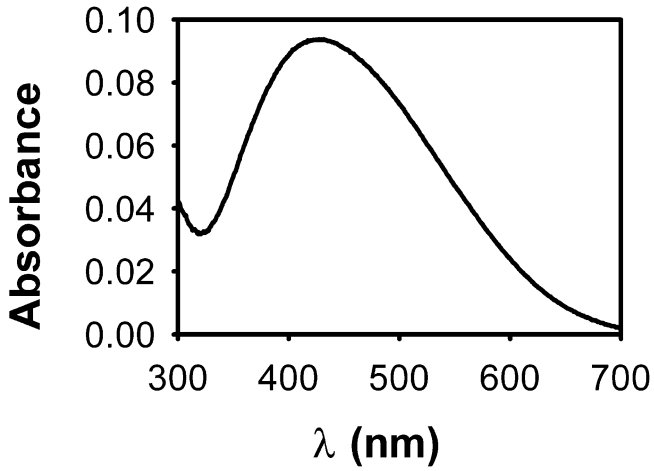

Figure 2. UV−vis spectrum recorded for the fresh AgNPs sol formed on anodic dissolution of Ag electrode in DMSO. The overpotential and duration were 100 V and 50 min, respectively.

2.4. Characterizations. Powder X-ray diffractograms (XRD) on the dried precipitate were recorded with a JEOL JDX- 8030 X-ray diffractometer having Cu Kα source (40 kV and 20 mA). Samples were prepared by sprinkling the dried powder over pregreased glass slides. The diffractograms were recorded between 20° and 70° with a scan rate of 2.0 s per step (0.05 step).

For routine characterization, UV−vis (Shimadzu UV-2401PC) spectra were recorded for the sols at the stipulated time intervals. Steady-state photoluminescence (PL) spectra were recorded at room temperature, using a Shimadzu RF-5301PC spectrofluorometer. The excitation wavelength (λ_{ex}) was fixed at 300 nm and emission spectra were recorded between 300 and 900 nm.

FTIR spectroscopy measurements were carried out with a Shimadzu FTIR 4200 spectrophotometer. For that, ca. 10 mg of the dried sample was mixed with ca. 100 mg of spectroscopic-grade potassium bromide, and the resultant suspension was mixed thoroughly by using a mortar and pestle. A small portion of the sample was pressed into a transparent homogeneous pellet at ca. 20 kpsi. The spectra were recorded on transmittance mode over 25 scans from which the background spectrum was automatically subtracted.

Transmission electron micrographs (TEM) on NPs were recorded with a Philips CM200 transmission electron microscope. A droplet of the sol was dried on carbon-coated TEM grid and the measurements were carried out at 88 kV. To understand the surface composition further, the vacuum-dried traces of AgNPs precipitate were subjected to thermal analyses in N_2 atmosphere. Isothermal heating of these samples was carried out in a homemade tube furnace under inert atmosphere.

3. Results and Discussions

3.1. Formation and Characterization of AgNPs in DMSO. On applying a potential difference of 100 V between silver electrodes immersed in DMSO, the electrochemical dissolution of silver anode took place, which led to the formation of pale yellow sol. Figure 2 shows the absorption spectrum recorded on such freshly prepared sol. A peak at 425 ± 5 nm seen in the spectrum is assigned to the surface plasmon resonance (SPR)

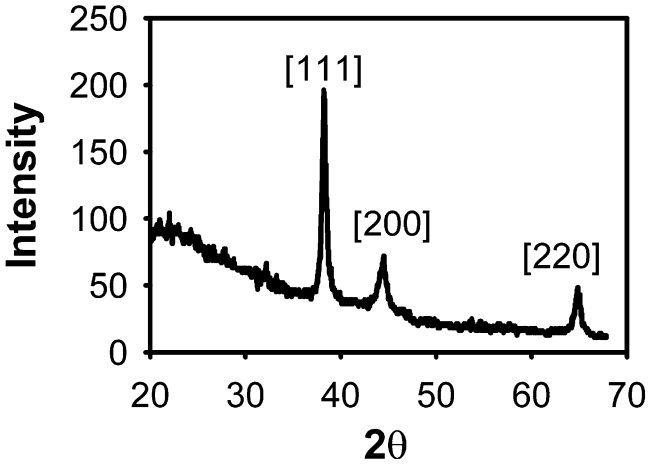

Figure 3. X-ray diffractogram recorded on a vacuum-dried sample extracted from the sol. The diffractogram is indexed by using JCPDS file 4-783.

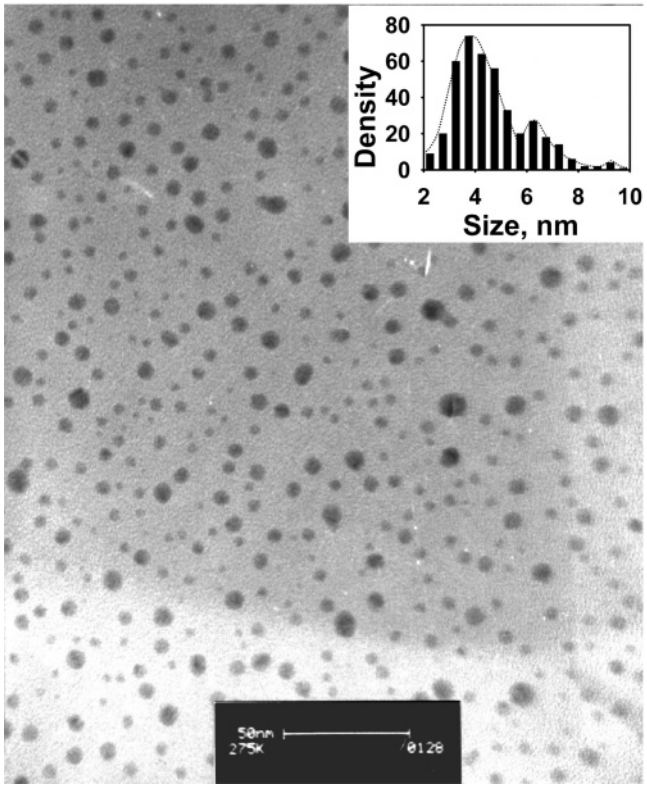

Figure 4. Low-resolution TEM image recorded at 88 kV for the drop-casted AgNPs. The time duration between preparation and measurements was ca. 24 h. The histrogram for the particle size distributions is given in the inset.

band for silver,[26] which suggested the formation of AgNPs in the solution.

To confirm the crystallographic phase, the X-ray diffractogram (XRD) was recorded on the dried sample as shown in Figure 3. The major peaks at 38.4°, 44.4°, and 64.6° fitted faithfully with the one reported for the cubic phase of silver. The value of the lattice constant was calculated to be 4.0688 ± 0.0049 Å, which matches well with 4.0862 Å, the value reported for silver.[27] A large line width of the peaks is attributed to the small crystallite size. By using the Scherrer equation, the average particle size was estimated to be about 5 nm.

A typical low-resolution TEM image obtained for the sol, drop casted onto TEM grid is given in Figure 4. In the micrograph, particles appear to be spherical in shape. From the histogram (Figure 4 inset) one can group these particle size distributions into three sets, viz., 3.75 ± 0.8, 6.25 ± 0.5, and 9.25 ± 0.3 nm (hereafter, size 1, size 2, and size 3, respectively). If the bigger sizes are forming by a coalition of respective smaller counterparts, then the volume of the bigger particles should be the sum of the volumes of combining small particles, that is

TABLE 1: Correlation of the Particles Sizes Calculated with Eq 8

n'	no. of d_1	no. of d_2	d_3, nm
0	0	3	9.01
1	5	2	9.09
2	10	1	9.17
3	15	0	9.25
4	20	−1	9.32
5	25	−2	9.40

$$V = nV_1 + mV_2 + l\,V_3 + ... \tag{1}$$

where, subscripts 1, 2, 3, ... indicate smaller particles having radii r_1, r_2, r_3, ..., respectively. n, m, and l are integers, which indicate the number of a given size of particles being combined. Here, density is assumed to be constant, throughout the size range.

Since AgNPs prepared were spherical, eq 1 simplifies to

$$\frac{4}{3}\pi R^3 = n\frac{4}{3}\pi {r_1}^3 + m\frac{4}{3}\pi {r_2}^3 + l\frac{4}{3}\pi {r_3}^3 + ... \tag{2}$$

$$R^3 = n{r_1}^3 + m{r_2}^3 + l\,{r_3}^3 + ... \tag{3}$$

For example, if n number of same size particles (say, of the type 1) combine to form a bigger one, then the equation further simplifies to

$$R^3 = n{r_1}^3 \tag{4}$$

$$R = \sqrt[3]{n}\,r_1 \tag{5}$$

$$r_1 = \frac{R}{\sqrt[3]{n}} \tag{6}$$

or

$$d_1 = \frac{D}{\sqrt[3]{n}} \tag{7}$$

where d_1 and D are dimeters of particle 1 and bigger particles, respectively. If the bigger particles are formed due to a coalition of smaller ones in the same size distribution, then the size of the bigger one can be correlated with eq 7.

For example, correlation between size 1 and size 3 fits well in the following relationship: 3.75 nm $\sqrt[3]{15}$ = 9.25 nm. That means size 3 is formed by a combination of 15 size 1 particles. This works well for other combinations also. For example, 3.75 nm$\sqrt[3]{5}$ = 6.41 nm, which matches well with 6.25 nm (size 2). The formation of size 3 can also be explained by coalition of two medium-sized particles (size 2), that is, 6.25 nm$\sqrt[3]{3}$ = 9.01 nm. More correlations in details are tabulated in Table 1. In fact, the rational relationship among these size distributions can be summarized by following empirical equation

$$5{d_1}^3 n' + (3 - n'){d_2}^3 = {d_3}^3 \tag{8}$$

where d_1, d_2, and d_3 are three sizes of particles and n' is an

integer having values of 0, 1, 2, 3, ... This analysis supports the nanoparticle formation model by Reetz et al. in which formation of higher sized NPs was explained on the basis of coalition of smaller clusters.[19] The average of all these size is about 6.6 nm, which is quite close to the value obtained by the Scherrer equation, that is ca. 5 nm.

3.2. Mechanism of NPs Formation. The exact mechanism for the NPs formation by the anodic dissolution of the electrode is not yet clearly understood. In case of Pd nanoparticles, Reetz et al. proposed the formation of charged Pd clusters: Pd_n^{m+} at the anode, which migrate and discharge at the cathode to form Pd^0 clusters, which were subsequently associated and stabilized by tetraalkylammonium salts.[19] A similar explanation was given by Sanchez et al. about the formation of AgNPs by anodic dissolution methods.[24] The charge balance in the electrode reactions has been explained on the basis of oxidation and reduction of M and M_n^{m+} clusters at the anode and the cathode, respectively. We also observed the black Ag deposit at the cathode irrespective of the nature of the cathode (either Pt or Ag), which is in concordance with the observation made by Reetz et al. Though it explains the electrophoretic migration and discharge of clustered ions to the cathode, it does not explain the nature of the electrochemical reaction that occurs at the cathode, especially when the first few clusters form near the anode. At that instant, the cluster ions are forming at the anode but have not yet migrated to the cathode to become neutralized. If the Ag anode becomes oxidized, then there ought to be reduction taking place at that instant at the cathode besides the Ag_m^+ reduction. In the Reetz et al. experiments, reduction/oxidation of solvent molecules at electrodes is ruled out as the applied potential difference was just 1−2 V. Thus, it cannot be explained unless reduction of tetraoctylammonium bromide at the cathode is assumed. Moreover, it would be less likely to form a complex of positively charged tetraalkylammonium cation with the M_n^{m+} cluster due to unfavorable columbic interaction between them. In the later stage, the simultaneous reduction reaction of M_n^{m+} and tetraalkylammonium ions at the cathode might be taking place, which leads to capped clusters in the case of the Reetz and Sanchez experiment.

In our case, electrolysis was carried out at 100 V, which was well above the equilibrium potential. Moreover, no capping agents or supporting electrolyte was added. Nevertheless, AgNP sols were obtained. This suggests that DMSO might be undergoing a redox reaction, which maintained the charge balance in the electrochemical reaction. Simultaneous reduction of DMSO and Ag_n^{m+} on the cathode may facilitate formation of DMSO complex on the particle surface, which might be responsible for an extraordinary solution stability of the particles. It would be similar to that of the formation of metal alkoxides on anodic dissloution of Fe, Co, and Ni in aprotic solvents or in dry alcohols.[28]

Recently, we have reported the formation of CdS nanoparticles prepared in DMSO, which are stable due to the formation of the Cd(II)-DMSO complex on the particle.[29] Moreover, DMSO is known to form a series of chain-like or square-structured stable complexes on the Au and Ag surface, in the presence of I^-.[30−32] It was established that I^- oxidizes to I_2, which leads to the formation of the charge transfer complex. This implies that DMSO undergoes a reduction reaction, which forms the complex with AgNPs. In the present experiments, the formation of the complex is most probably facilitated by an electron-transfer reaction at the cathode.

To ascertain the role of DMSO in AgNPs stabilization, electrolysis was carried out in DMF at exactly identical conditions. Though the particle formations were observed after the electrolysis, the sols so formed were unstable and precipitated within a few hours.

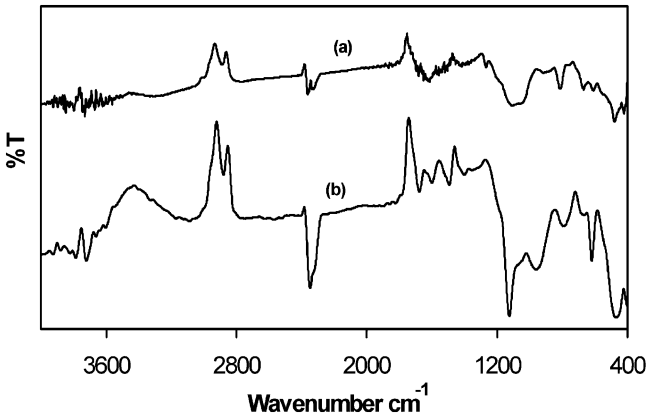

Figure 5. FTIR spectra recorded on (a) prestine DMSO and (b) KBr pallet of AgNPs flocculated from sol.

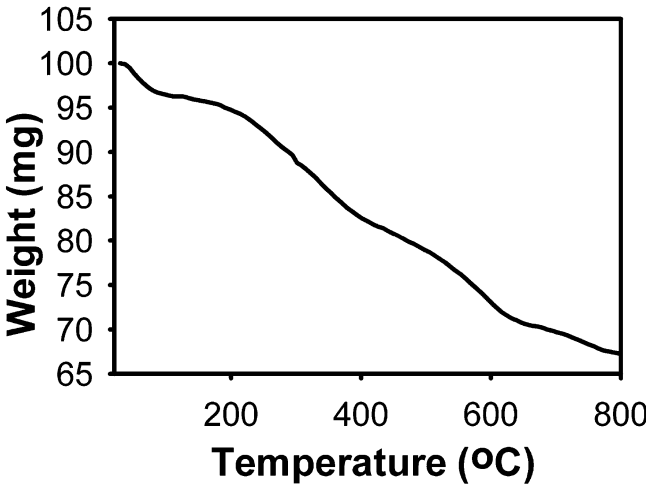

Figure 6. TGA recorded for a dried sample in N_2 atmosphere. The scan rate was 10 deg/min.

To confirm the formation of the DMSO complex on the particle surface, FTIR spectra were recorded (Figure 5b) on the sample. Additional prominent peaks at 470, 603, 805, 1108, and 1262 cm^{-1} were observed besides characteristic bands belonging to free DMSO (refer to Figure 5a). A broad band, in the range of 1050 to 1100 cm^{-1} due to S═O stretching in free DMSO, is split into 1135 and 981 cm^{-1} along with a shoulder at 1056 cm^{-1} for free DMSO. Peaks at 1135 and 981 cm^{-1} have been attributed to the bonding of DMSO with metal through sulfur and oxygen moieties, respectively. Formation of such a chain complex of DMSO has already been confirmed on Au and Ag surface by STM, capacitance, and electrochemical measurements.[30]

3.3. Thermal Analysis. To understand the surface composition of the Ag-DMSO further the precipitate was subjected to thermogravometric analysis (TGA) under nitrogen atmosphere. Figure 6 shows a thermogram recorded on a vacuum-dried sample. Three prominent weight loses were observed at the onset temperatures 70, 195, and 400 °C. Weight loss that onset at ca. 70 °C and endset at 100 °C has been attributed to the physical desorption of a moisture from the surface of AgNPs. The major weight loss that onset at 195 °C matches well with the boiling point of DMSO and is attributed to the physical desorption DMSO from the particle surface. The weight loss that onsets at 460 °C could be attributed to the decomposition of Ag(I)DMSO

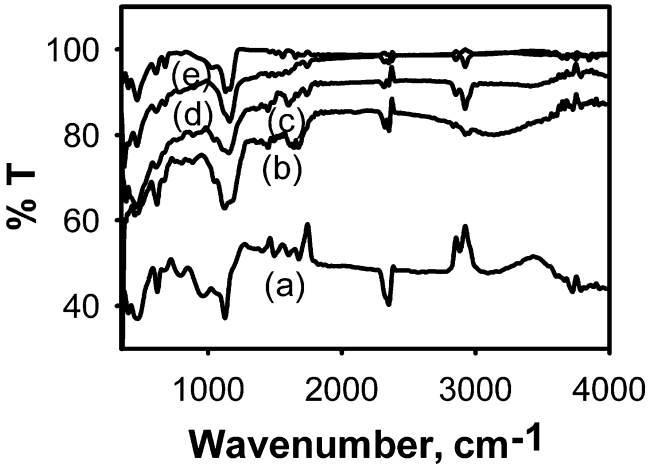

Figure 7. FTIR spectra recorded on AgNPs after annealing at (b) 200, (c) 300, (d) 400, and (e) 500 °C. (a) The FTIR spectrum for the controlled sample.

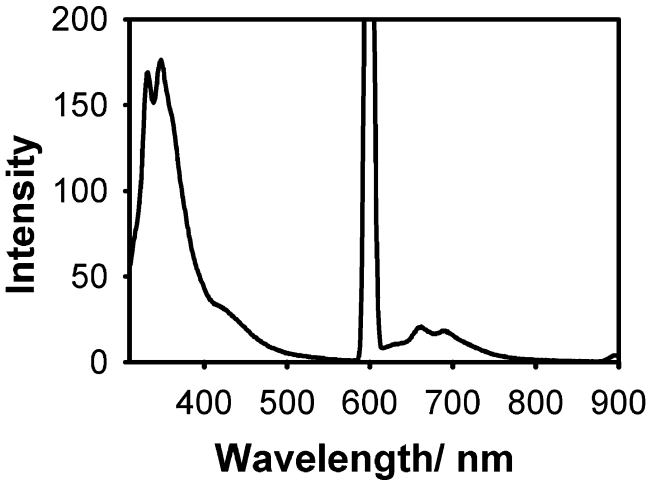

Figure 8. Emission spectra recorded for AgNPs in DMSO. The excitation wavelength was 300 nm.

complex. Similar obervations were reported in case of CdS nanoparticles prepared in DMSO.[29]

To resolve the processes occurring at 400 °C, IR spectra were recorded for AgNPs followed by isothermal heating at 200, 300, 400, and 500 °C (Figure 7). The peaks at 1135 and 1050 cm^{-1} which were assigned to Ag(I)DMSO complex are prominently seen up to 300 °C. With isothermal heating at and above 400 °C both peaks were diminished. There is no apparant difference in the spectral feature upon further heating at 500 °C. Thus, this set of experiments emphasize the formation of Ag(I)DMSO complex on the particle surface.

3.4. Steady-State Photoluminescence (PL) Measurements. Figure 8 depicts PL spectra recorded (λ_{exc} = 300 nm) on the sols. A sharp peak at 333 nm and a strong peak at 600 nm were attributed to the first-order Raman scattering and second-order Rayleigh scattering, respectively. Besides these, prominent emissions at 349, 421, 664, and 693 nm are seen in the spectrum. Silver clusters of the size of order of 5−9 nm are not known to give PL.[33] Therefore, these emissions were attributed to the DMSO complex formed on the particle surface. Interestingly, similar complex formed in the case of CdS nanoparticles prepared in DMSO was known to give emissions at 346 and 686 nm, which are quite close to the present observation.[34]

4. Conclusions

Silver nanoparticles without any surface stabilizing additives have been prepared by electrochemical dissolution of silver anode in DMSO. The formation of silver nanoparticles has been confirmed by XRD, UV−vis, and TEM. Three types of size distribution are seen in the micrograph, which could be explained on the basis of droplet coalition model. High overpotential (100 V) seems to facilitate the formation of DMSO complex on the particle surface, which might be responsible for the solution stability. The existence of such a complex has been confirmed by FTIR, PL, and thermal analysis. The advantages of the present methodology for the preparation of AgNPs are 3-fold:(1) extremely pure sol of monodispersed AgNPs can be prepared by a very simple setup, (2) the procedure can be scaled up for large-scale synthesis of nanoparticles, and (3) being free from surface capping agents, e.g., thiols or amines, these particles have potential applications in the field of catalysis.

Acknowledgment. We thank TIFR and RSIC, IIT, Mumbai for XRD and TEM facilities, respectively. We also thank Dr. Nanda S. Haram for useful discussions.

Supporting Information Available: UV−visible spectra for Ag NPs synthesized at different potential difference. This material is available free of charge via the Internet at http://pubs.acs.org.

References and Notes

(1) Sun, Y.; Xia, Y. *Science* **2002**, *298*, 2176.
(2) Jana, N. R.; Gearheart, L.; Murphy, C. J. *Chem. Commun.* **2001**, *7*, 617.
(3) Yao, J. L.; Pan, G. P.; Xue, K. H.; Wu, D. Y.; Ren, B.; Sun, D. M.; Tang, J.; Xu, X.; Tian, Z. Q. *Pure. Appl. Chem.* **2000**, *72*, 221.
(4) Hu, J. T.; Odom, T. W.; Lieber, C. M. *Acc. Chem. Res.* **1999**, *32*, 435.
(5) Wang, J.; Liu, G.; Merkovi, A. *J. Am. Chem. Soc.* **2003**, *125*, 3214.
(6) McConnell, W. P.; Novak, J. P.; Brousseau, L. C.; Fuierer, R. R.; Tenent, R. C.; Feldheim, D. L. *J. Phys. Chem. B* **2000**, *104*, 8925.
(7) Ghosh, K.; Maiti, S. N. *J. Appl. Polym. Sci.* **1996**, *60*, 323.
(8) Andres, P. R.; Bielefeld, J. D.; Henderson, J. I.; Janes, D. B.; Kolagunta, V. R.; Kubiak, C. P.; Mahoney, W.; Osifchin, R. G.; Reifenberger, R. *Science* **1996**, *273*, 1960.
(9) Murray, C. B.; Sun, S.; Doyle, H.; Betley, T. *Mater. Res. Soc. Bull.* **2001**, *26*, 985.
(10) Forster, S.; Antonietti, M. *Adv. Mater.* **1998**, *10*, 195.
(11) Andres, P. R.; Bein, T.; Dorogi, M.; Feng, S.; Henderson, J. I.; Kubiak, C. P.; Mahoney, W.; Osifchin, R. G.; Reifenberger, R. *Science* **1996**, *272*, 1323.
(12) Zhao, S.; Chen, S.; Wang, S.; Li, D.; Ma, H. *Langmuir* **2002**, *18*, 3315.
(13) Jana, N. R.; Wang, Z. L.; Pal, T. *Langmuir* **2000**, *16*, 2457.
(14) Lee, P. C.; Miesel, D. J. *J. Phys. Chem.* **1982**, *86*, 3391.
(15) Creigton, J.; Blatchford C.; Albercht, M. *J. Chem. Soc., Faraday Trans.* **1979**, *75*, 790.
(16) Brust, M.; Walker, M.; Bethell, D.; Shiffrin, D. J.; Whyman, R. *J. Chem. Soc., Chem. Commun.* **1994**, 801.
(17) Pastoriza-Santos, I.; Liz-Marzan, L. M. *Pure Appl. Chem.* **2001**, *72*, 1−2, 83.
(18) Rodriguez-Gattorno, G.; Diaz, D.; Rendon, L.; Hernandez-Segura, G. O. *J. Phys. Chem. B.* **2002**, *106*, 2482.
(19) Reetz, M. T.; Helbig, W. *J. Am. Chem. Soc.* **1994**, *116*, 7401.
(20) Yin, B.; Houyi, M.; Shuyun, W.; Shenhao, C. *J. Phys. Chem. B* **2003**, *107*, 8898.
(21) Ma, H.; Yin, B.; Wang, S.; Jiao, Y.; Pan, W.; Huang, S.; Chen, S.; Meng, F. *ChemPhysChem* **2004**, *5*, 68.
(22) Singaud, M.; Li, M.; Chardon-Noblat, S.; Jos Cadete Santos Aires, F.; Soldo-Olivier, Y.; Simon, J.-P.; Renouprez, A.; Deronzier, A. *J. Mater. Chem.* **2004**, *14*, 2606.
(23) Socol, Y.; Abramson, O.; Gedanken, A.; Meshorer, Y.; Berenstein, L.; Zaban, A. *Langmuir* **2002**, *18*, 4736.
(24) Rodrigues-Sanchez, L.; Blanco, M. C.; Lopez-Quintela, M. A. *J. Phys. Chem. B* **2000**, *104*, 9683.
(25) Yu, Y. Y.; Chang, S. S; Lee, C. L.; Wang, C. R. C. *J. Phys. Chem. B* **1997**, *101*, 6661.

(26) Kelly, K. L.; Coronado, E.; Zhao, L. L.; Schatz, G. C. *J. Phys. Chem. B* **2003**, *107*, 668.
(27) Joint Committee of Powder Diffraction Standard. JCPDS File 4-783.
(28) Coiper, A. M.; Pletcher, D.; Walsh, F. C. *Chem. Rev.* **1990**, *90*, 837.
(29) Wankhede, M. E.; Haram, S. K. *Chem. Mater.* **2003**, *15*, 1296.
(30) Siv, S. K.; Andrew, G. A. *Phys. Chem. Chem. Phys.* **2001**, *3*, 3325.
(31) Shen, A.; Pemberton J. E. *J. Electroanal. Chem.* **1999**, *479*, 21.
(32) Shen, A.; Pemberton J. E. *J. Electroanal. Chem.* **1999**, *479*, 32.
(33) Peyser, L. A.; Vinson, A. E.; Bartko, A. P.; Dickson, R. M. *Science* **2001**, 103
(34) Elbaum, R.; Vega, S.; Hodes, G. *Chem. Mater.* **2001**, *13*, 2272.